

DETERMINATION OF THE ORBITAL ELEMENTS OF ASTEROID 1993 MO

S. Chen, E. Marshall, N. Wei - Team 1

July 23rd, 2022, Summer Science Program, New Mexico Tech Campus

Abstract

Near-Earth asteroids, or NEAs, have the potential to cross Earth's orbit and collide with the planet, which is why it is vital to understand their orbits. We determined the orbital elements of one such NEA, 1993 MO. We located the asteroid, gaining positional data after performing image reduction, astrometry, and photometry on our images from four observations. With these initial positions, we programmed the method of Gauss and iterated our data through it. Then we coded a Monte Carlo simulation to estimate our error level by obtaining our measurements' mean and standard deviation. After 70 iterations, our values for the magnitudes of the central position and velocity vectors converged to approximately 1.2725 au and 0.016848 au/day, respectively. From this, we determined the orbital elements of 1993 MO to be $a = 1.6 \pm 0.5 \text{ au}$, $e = 0.22 \pm 0.07$, $i = 23 \pm 4^\circ$, $\omega = 170 \pm 80^\circ$, $\Omega = 110 \pm 80^\circ$, and $M = 1.2 \pm 50^\circ$. We discovered that 1993 MO is in the Amor family and will not cross Earth's orbit[1].

Introduction

In determining the orbit of a near-Earth asteroid, one challenge is finding a three-dimensional orbit in space based on limited observations from Earth. To overcome this challenge, we made four observations of 1993 MO spaced out through a time interval of 17 days, utilized astrometry and aperture photometry to obtain its position at these times, and used Python to code the method of Gauss to compute its orbital elements from this information. We

hypothesized that our results would be close to the theoretical predictions offered by the JPL Horizons web application[2].

```
2459784.750000000 = A.D. 2022-Jul-24 06:00:00.0000 TDB
EC= 2.206255664784977E-01 QR= 1.267344384015169E+00 IN= 2.263954286354251E+01
OM= 1.114761607416965E+02 W = 1.673417675564451E+02 Tp= 2459782.007721829228
N = 4.753148025942848E-01 MA= 1.303445407398907E+00 TA= 2.092810638847729E+00
A = 1.626104641755872E+00 AD= 1.984864899496576E+00 PR= 7.573927806058372E+02
```

Figure 1- Predicted orbital elements as shown in JPL Horizons

If we could not locate the asteroid in the photographs from an observation, that observation would have to be rejected. And if iterations in the method of Gauss would not converge on an acceptable value, or if the results we found were substantially different from the predictions offered by JPL Horizons, our experiment would have failed.

The orbital elements are six parameters that describe the orbit of an asteroid or any other object. The semimajor axis (a) is a component of an ellipse, described by the equation

$\frac{x^2}{a^2} + \frac{y^2}{b^2} = 1$, which gives the size of the asteroid's orbit in astronomical units (au). By

arranging the vis-viva equation₂, one can find $a = \left(\frac{2}{|\vec{r}|} - \frac{\dot{\vec{r}} \cdot \dot{\vec{r}}}{\mu} \right)^{-1}$, where $\mu = k^2$ and k is a

constant. The eccentricity (e) describes how elongated the elliptical orbit is, where a circular orbit would have $e = 0$ and a parabolic orbit has $e = 1$. The eccentricity can be described by

$e = \sqrt{1 - \frac{|\vec{r} \times \dot{\vec{r}}|^2}{\mu a^2}}$.₃ The inclination (i) is the angle between the plane of the asteroid's orbit

and the plane of the ecliptic, measured between 0° and 180° , described by $\cos i = \frac{h_z}{|\vec{h}|}$.₄ The

longitude of the ascending node (Ω) is the angle between the vernal equinox and the ascending node, measured eastward in the ecliptic plane from 0° to 360° . It is fully described by the

equations $\sin \Omega = \frac{h_x}{h \sin i}$ and $\cos \Omega = -\frac{h_y}{h \sin i}$.⁴ The argument of the perihelion (ω) is the angle between the asteroid's ascending node and its perihelion, measured eastward in the asteroid's orbital plane from 0° to 360° and described by $\omega = U - v$.⁵ Finally, the mean anomaly (M) is the angular position measured from the center of the orbit eastward from the perihelion point from 0° to 360° , of a test mass on a circular orbit with a radius equal to the semimajor axis. It is described by $M = E - e \sin E$ at the time of the central observation, or $M(t_0) = M + n(t_0 - t_2)$, where t_0 is some reference time in the recent past.⁶

The method of Gauss (MoG) is an iterative method used to approximate the asteroid's position and velocity vectors, \vec{r} and $\dot{\vec{r}}$ for the central observation, given three sets of the asteroid's $\{t_i, \alpha_i, \delta_i\}$ from three observations, which can then be used to calculate the six orbital elements. After picking an initial r_2 value using the scalar equation of Lagrange, we used that number to get initial values for \vec{r}_2 and $\dot{\vec{r}}_2$, then used a truncated Taylor series expansion of \vec{r} about the central value to iteratively improve upon the central position and velocity vectors until the current and previous values of r_2 varied by less than the tolerance limit of 1×10^{-12} . We estimated the error of our calculated orbit using a Monte Carlo simulation, where we first used the uncertainty values obtained from the astrometry for each right ascension and declination of each date to create a set of 10,000 numbers with a normal distribution centered at each right ascension or declination and a standard deviation that matched the uncertainty values accordingly. These numbers provided predicted right ascension and declination numbers for us to simulate using the method of Gauss procedure. We performed the method of Gauss procedure using each of these simulated right ascension and declination numbers to obtain our orbital

elements, iterating 10,000 times. After obtaining a list of these orbital elements from the simulation, we found the uncertainties of each orbital element.

Equipment and Procedure

Before we used the telescope to obtain our data, we first obtained an ephemeris from the Jet Propulsion Laboratory's Horizons System. It generated predictions for the approximate right ascension, declination, altitude, and apparent magnitude of our asteroid during each observing session, using 1993 MO as our target body and the Minor Planet Center code for Etsorn Observatory, 719, as our observer location. We used those predictions to obtain a focus star near our asteroid and a finding chart of its location using the software SAOImageDS9[3].

For observations, we used a C-14 model telescope with a diameter of 365mm, a focal length of 3,911mm, and an equatorial mount, as well as a SBig STL-11000M camera with a 4,008 by 2,745-pixel array[4]. During each observation, we slewed the telescope to the predicted right ascension and declination of our asteroid at the middle of our observation session. After ensuring that the images matched our finding charts, we focused the camera with a Bahtinov focus mask. Next, using the software SkyX and an SBig STL-11000M camera, we used 3x3 binning and a 60-second exposure time to take 3 sets of 5 light images per observation shift, taking each set about 20 minutes apart. In addition, we took 11 biases (images with a closed shutter and zero exposure time) and 9 darks (images with a closed shutter and a 60-second exposure time) per observation shift.

Data

The following data table is a collection of the results of our astrometry and aperture photometry, based on data collected on four different nights.

Observation date/time (UTC)	Asteroid Position (α , δ)	RMS Uncertainty (arcseconds)	Apparent magnitude	SNR (Signal to Noise Ratio)
6/30/2022 07:41:57	(15:21:05.19, +16°17'36.1'')	(± 0.19 , ± 0.4)	17.0 V	4.07
6/30/2022 08:21:23	(15:21:05.20, +16°16'00.4'')	(± 0.2 , ± 0.3)	16.3 V	9.20
7/7/2022 05:26:40	(15:22:42.5, +09°25'34.3'')	(± 0.4 , ± 0.4)	16.9 R	5.86
7/7/2022 05:44:09	(15:22:42.3, +09°24'45.6'')	(± 0.3 , ± 0.5)	17.5 R	4.23
7/8/2022 05:21:50	(15:23:10.0, +8°24'22.0'')	(± 1.2 , ± 0.4)	16.7 R	5.90
7/8/2022 05:50:18	(15:23:10.3, +08°23'09.1'')	(± 0.3 , ± 0.2)	16.6 R	9.32
7/16/2022 03:50:51	(15:28:36.3, +00°12'54.4'')	(± 0.5 , ± 1.1)	17.6 R	6.47
7/16/2022 04:11:44	(15:28:37.1, +00°11'52.0'')	(± 0.7 , ± 0.8)	17.0 R	6.90

Figure 2- Table of asteroid data and data analysis taken

Each row of this data table represents data from a single image. The first column is the time the image was taken in UTC. The second column is the right ascension and declination of the asteroid. The third column is the root mean squared uncertainty on our right ascension and declination. The fourth column is the visual magnitude of 1993 MO and the filter used to take the observation, with R representing the clear filter and V representing green/visual. The fifth column is the signal-to-noise ratio (SNR).

Analysis

After collecting data, we reduced the images using the software AstroImageJ[5], subtracting the biases and dark, and dividing out the flats. Then we aligned the images and blinked through them in a sequence to find the asteroid moving through the photographs. Once we located the asteroid, we performed astrometry using the website nova.astrometry.net[6] and AstroImageJ to estimate 1993 MO's right ascension and declination from the cartesian values on the images. Then, we ran the corrected fits images through a RMS (root mean square) program of the astrometry to find the uncertainties on the right ascensions and declinations. Finally, we created Python programs to perform aperture photometry on two images per observation date. We used the AAVSO Photometric All Sky Survey catalog and the software DS9 to determine the signal and apparent magnitudes for 5 reference stars per image, then performed a linear regression to determine the apparent magnitude of 1993 MO.

	S. Chen	N. Wei	E. Marshall	Uncertainty
Semi-major (AU)	1.6	1.6		0.5
Eccentricity	0.22	0.22		0.07
Inclination(°)	23	23		4
Longitude of Ascending Node (°)	110	110		80
Argument of Perihelion (°)	170	170		80
Mean Anomaly¹ (°)	1.4	0.9		50

Figure 3- Table of orbital elements generated by our OD code

¹ At 7/24/2022 6:00 UTC 2459784.75 JD

	Semi-major (AU)	Eccentricity	Inclination (°)	Longitude of Ascending Node (°)	Argument of Perihelion (°)	Mean Anomaly² (°)
JPL Horizons	1.62610464 1755872	.2208491331 781172	22.639480 0830482	167.28327 51810007	111.493544 5016715	1.3034454 07398907

Figure 4- Table of orbital elements generated by JPL Horizons

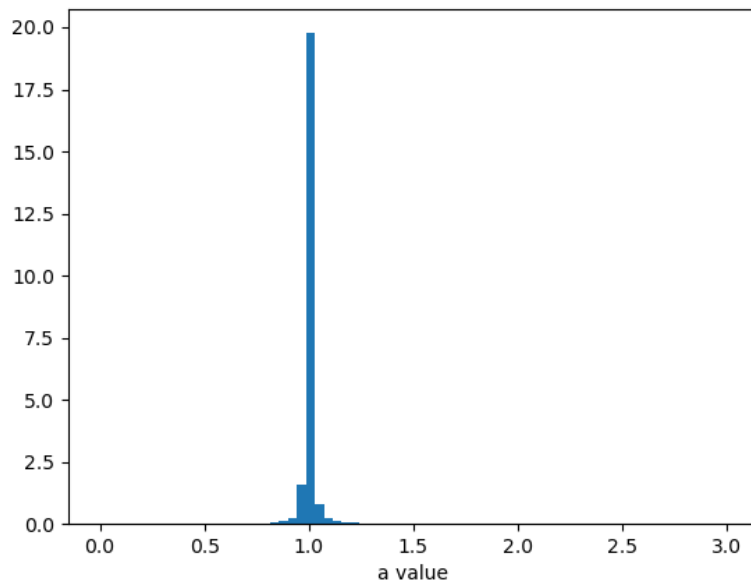


Figure 5 - Monte Carlo graph for semi-major axis

² At 7/24/2022 6:00 UTC 2459784.75 JD

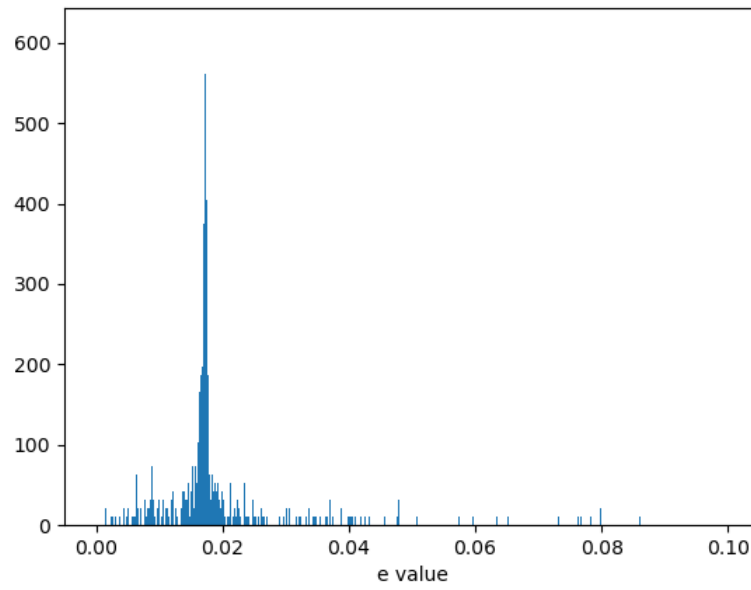


Figure 6 - Monte Carlo graph for eccentricity

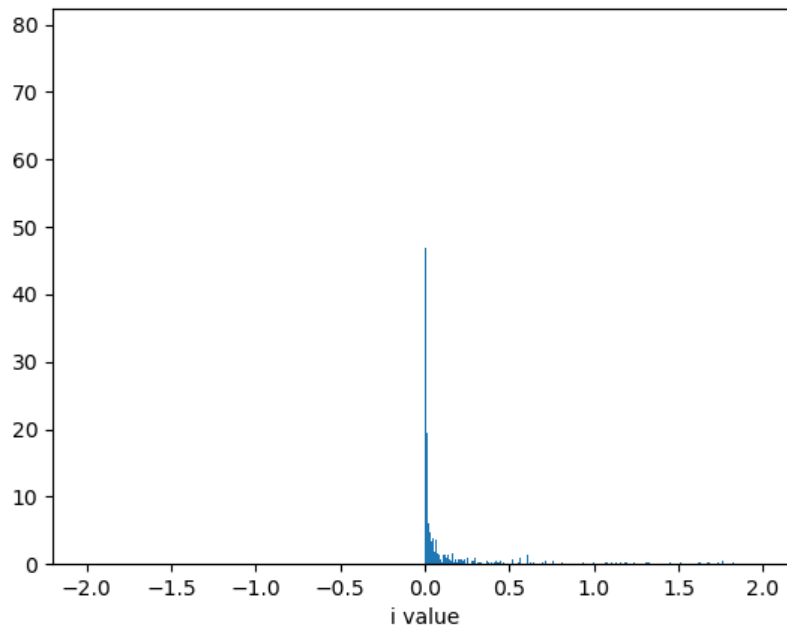


Figure 7 - Monte Carlo graph for inclination

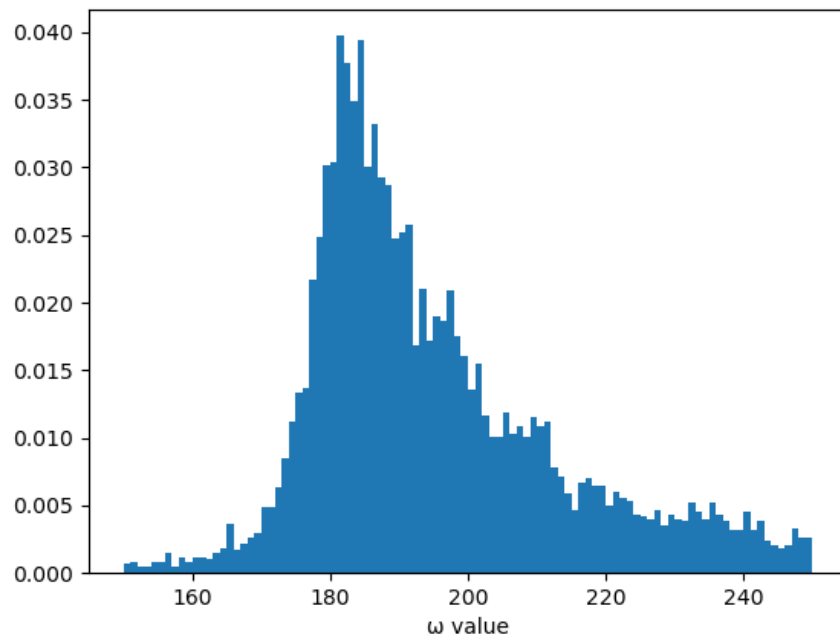


Figure 8 - Monte Carlo graph for argument of perihelion

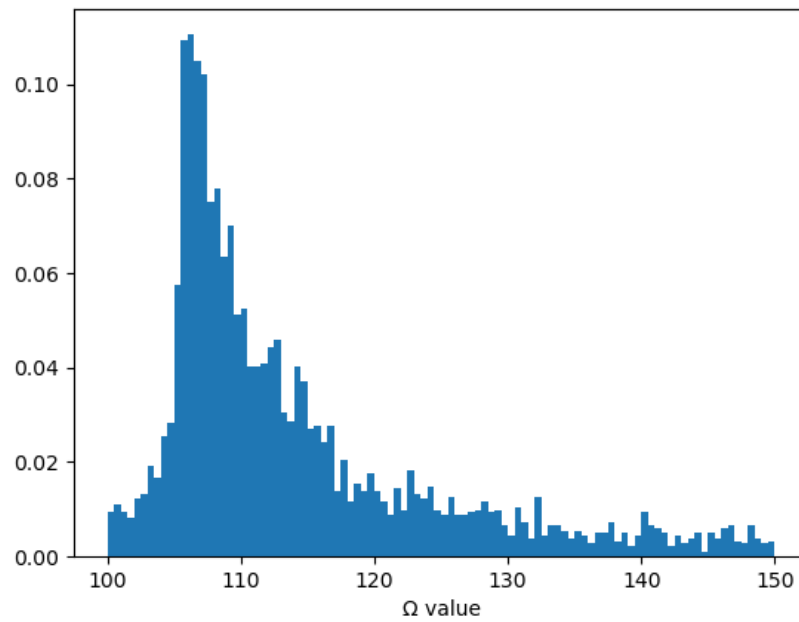


Figure 9 - Monte Carlo graph for longitude of ascending node

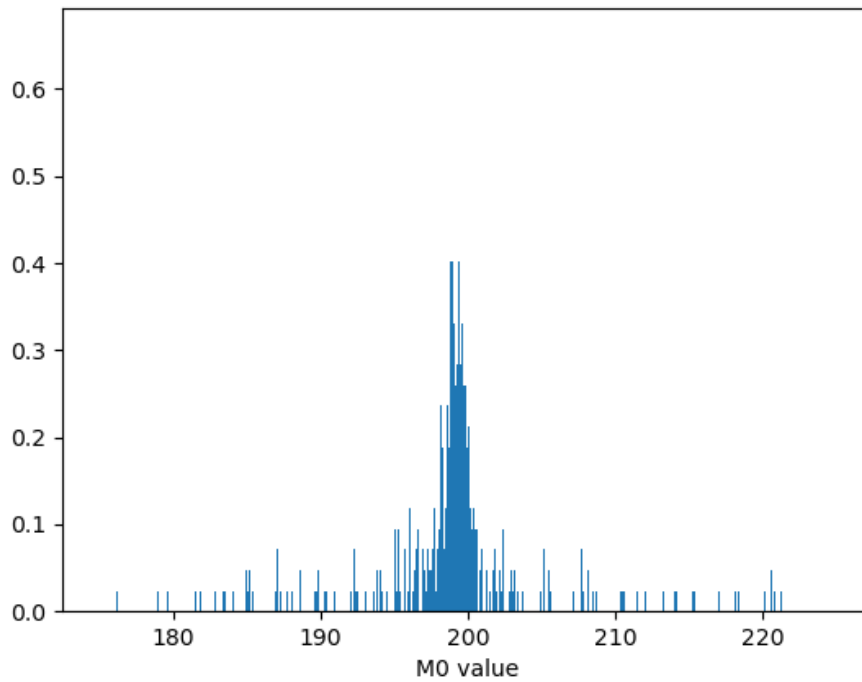


Figure 10 - Monte Carlo graph for mean anomaly

Our orbital elements agree, within uncertainty, with elements generated from JPL horizons, as seen in Figure 1. The asteroid 1993 MO is in the Amor family of asteroids that are outside Earth's orbit and inside Mars' orbit, with perihelions between 1.017 and 1.3 AU.

Conclusion

For the asteroid 1993 MO, we determined the orbital elements $a = 1.6 \pm 0.5au$, $e = 0.22 \pm 0.07$, $i = 23 \pm 4^\circ$, $\Omega = 110 \pm 80^\circ$, $\omega = 170 \pm 80^\circ$, and $M = 1.2 \pm 50^\circ$. JPL Horizons predicted

$a = 1.626 au$, $e = 0.2208$, $i = 22.64^\circ$, $\Omega = 111.5^\circ$, $\omega = 167.3^\circ$, and $M = 219.5^\circ$.

Therefore, our values for the orbital elements all agree, within uncertainty, to the predictions in our hypothesis. The accuracy of our results may have been affected by uncertainties in measurement, such as imprecision in measuring the exact second our observations were made, or

the exact right ascension and declination produced by astrometry. We conclude that, as an Amor family asteroid with a perihelion of greater than 1.05 au, 1993 MO will not cross Earth's orbit. For future experiments, we could select an Earth-crossing asteroid from the Apollo or Aten family and perform an orbit improvement using additional observations.

Acknowledgements

Thank you to Dr. Adam Rengstorf for giving us a foundation in observational astronomy.

Thank you to Dr. William Andersen for teaching us the math and physics behind the Method of Gauss.

Thank you to Kathryn Chan, Eric He, Benjamin Khoury, and Jessica Lee for assisting us with taking observations and debugging code.

References

- [1] NEO Program, Jet Propulsion Laboratory, California Institute of Technology, NASA (2002)
- [2] Horizons System, Jet Propulsion Laboratory, California Institute of Technology, NASA (2022)
- [3] SAOImageDS9, Smithsonian Astrophysical Observatory, Harvard University (2022)
- [4] A. Rengstorf (private communication)
- [5] AstroImageJ, ImageJ, National Institutes of Health (2022)
- [6] nova.astrometry.net, NSF, NASA (2022)

Appendices

1. Observational data as reported to the Minor Planet Center

COD 719

CON A. W. Rengstorf

CON [adamwr@pnw.edu]

OBS S. Chen, E. Marshall, N. Wei

TEL 0.36-m f/11 reflector + CCD

NUM 8

ACK Team 1 - 1993 MO

06569	C2022 06 30.32080 15 21 05.19 +16 17 36.1	17.0 V	719
06569	C2022 06 30.34818 15 21 05.20 +16 16 00.4	16.3 V	719
06569	C2022 07 07.22685 15 22 42.52 +09 25 34.3	16.9 R	719
06569	C2022 07 07.23899 15 22 42.31 +09 24 45.6	17.5 R	719
06569	C2022 07 08.22297 15 23 10.00 +08 24 22.0	16.7 R	719
06569	C2022 07 08.24326 15 23 10.30 +08 23 09.1	16.6 R	719
06569	C2022 07 16.16031 15 28 36.33 +00 12 54.4	17.6 R	719
06569	C2022 07 16.17481 15 28 37.12 +00 11 52.0	17.0 R	719

2. Vis-viva equation

$$\dot{\vec{r}} \cdot \dot{\vec{r}} = v^2 = \mu \left(\frac{2}{r} - \frac{1}{a} \right)$$

3. Eccentricity derivation

$$\frac{h^2}{\mu} = a(1 - e^2)$$

$$e = \sqrt{1 - \frac{h^2}{\mu a}}$$

$$\vec{h} = (\vec{r} \times \dot{\vec{r}})$$

4. Longitude of ascending node derivation

$$(h \sin i) \cos(90 - \Omega) = h_x$$

$$(h \sin i) \sin(90 - \Omega) = -h_y$$

5. Argument of the perihelion equations

$$U = \omega + v$$

$$\vec{r} \cdot \hat{n} = r \cos U$$

$$\vec{r} \cdot \hat{n} = \vec{r} \cdot (\cos \Omega \hat{i} + \sin \Omega \hat{j}) = x \cos \Omega + y \sin \Omega$$

$$\cos U = \frac{x \cos \Omega + y \sin \Omega}{r}$$

$$\hat{n} \times \hat{r} = \hat{n} \times \left(\frac{\vec{r}}{r}\right) = \frac{1}{r} [z \sin \Omega \hat{i} - z \cos \Omega \hat{j} - (x \sin \Omega - y \cos \Omega) \hat{k}]$$

$$\frac{z}{r} \sin \Omega = \sin U \sin i \sin \Omega$$

$$\sin U = \frac{z}{r \sin i}$$

$$r = \frac{a(1-e^2)}{1+e \cos v}$$

$$e \cos v = \left[\frac{a(1-e^2)}{r} - 1\right]$$

$$-e \dot{v} \sin v = -\frac{a(1-e^2)}{r^2} \dot{r}$$

$$e \sin v = \frac{a(1-e^2)}{h} \frac{\vec{r} \cdot \dot{\vec{r}}}{r}$$

6. Mean anomaly equations

$$r = a(1 - e \cos E)$$

$$\cos E = \frac{1}{e} \left(1 - \frac{r}{a} \right)$$

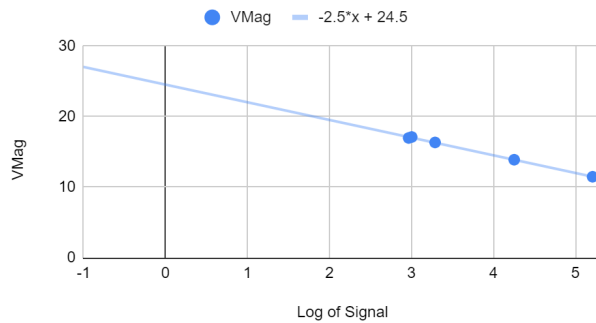
$$n = \sqrt{\mu/(a^3)} = k/(a^{3/2})$$

$$M(t_0) - M = n(t_0 - T) - n(t_2 - T) = n(t_0 - t_2)$$

7. Linear regressions for aperture photometry

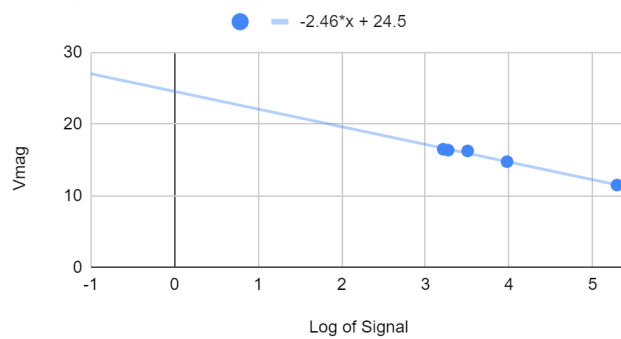
2022-06-30 07:41:57

VMag vs. Log of Signal



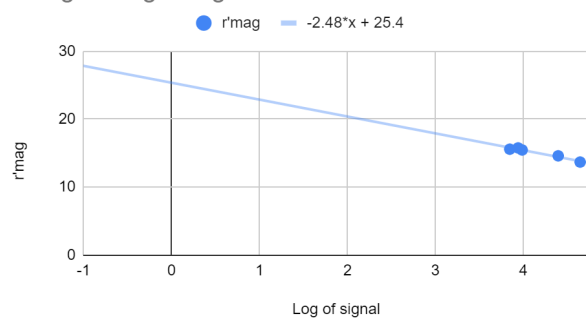
2022-06-30 08:21:23

Vmag vs. Log of Signal



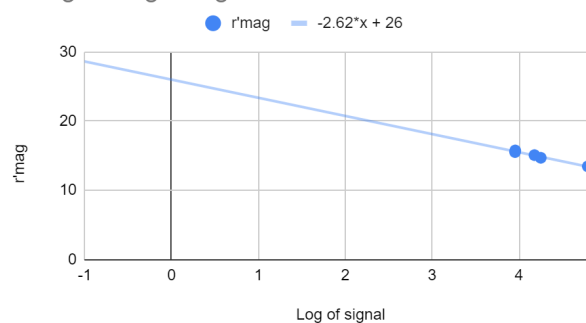
2022-07-07 05:26:40

r'Mag vs. log of signal



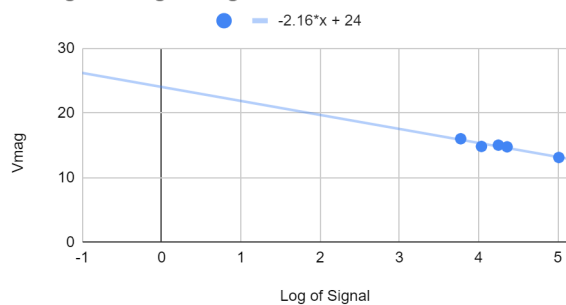
2022-07-07 05:44:09

r'Mag vs. log of signal



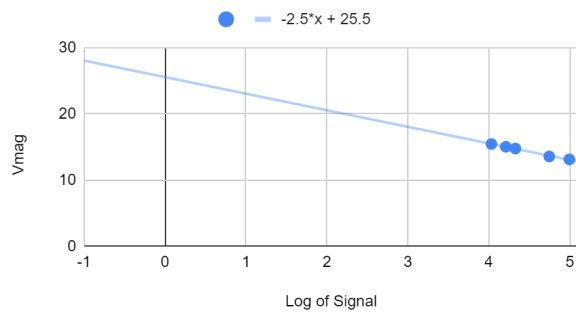
2022-07-08 05:21:50

Vmag vs. Log of Signal



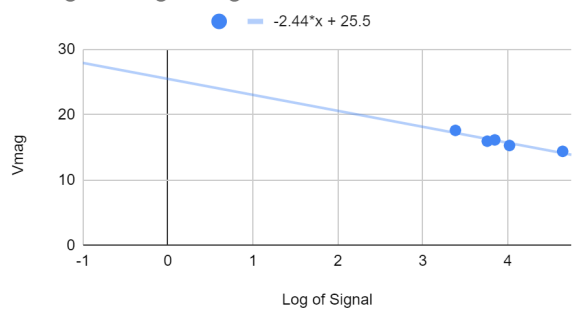
2022-07-08 05:50:18

Vmag vs. Log of Signal



2022-07-16 03:50:51

Vmag vs. Log of Signal



2022-07-16 04:11:44

Vmag vs. Log of Signal

